Polymer Whiskers of Poly(4-hydroxybenzoate): Reinforcement Efficiency in Composites with Polyamides

CHR. TAESLER,[1] H. WITTICH,[1] C. JÜRGENS,[1] K. SCHULTE,[1,*] and H. R. KRICHELDORF[2]

[1]Technical University Hamburg-Harburg, Polymer Composite Group, Denickestr. 15, D-21073 Hamburg, and
[2]University of Hamburg, Department of Macromolecular Science, Hamburg, Germany

SYNOPSIS

The reinforcing efficiency of polymer whiskers of poly(4-hydroxybenzoate) (PHB) in polyamide-6 (PA-6) and polyamide-11 (PA-11) composites was investigated by tensile testing, scanning electron microscopy (SEM), and density measurements. The composites were prepared by mixing the whiskers into the melts of the polyamides. Ductile and stiff PA-6-composites with different crystallinities of the PA-6-matrix were investigated. In the ductile PA-6 (low crystallinity) composites, the elastic modulus E and the yield stress σ_f increase more than twice at a whisker content of 2 vol %. The increase in E and σ_f in stiff PA-6 (high crystallinity) composites is not as pronounced as in the ductile PA-6 composites, but is still remarkably higher than in the PA-11 composites, which is about 1.2 times at a whisker content of 2 vol %. At higher whisker content, the PA-6 composites show the opposite of the PA-11-composite—no further increase in E and σ_f, which may be due to an agglomoration of whiskers in the high viscous PA-6 melt. The different tensile properties of the composites can be explained by SEM analysis of the fracture surfaces, which shows that the adhesion of PA-6 to the PHB whiskers is better than of PA-11. This is due to a higher number of hydrogen bonds between the PA-6 and the whisker surface. Density measurements show that the crystallinity of the polyamides is not affected by the PHB whiskers.

INTRODUCTION

The synthesis and the structural and morphological characterization of poly(4-hydroxybenzoate) (PHB), whose chemical structure is shown in Figure 1, has been a subject of investigations since the 1970s.[1-3] Under certain conditions, the polycondensation of monomers like 4-acetoxybenzoic acid in high boiling solvents leads to needlelike single crystals of PHB, also called PHB whiskers.[4-6] Their morphology is visualized by scanning electron microscopy (SEM), as shown in Figure 2. The PHB chains are fully extended into the direction of the long axis of the whisker.[7] PHB whiskers should therefore have a high stiffness and strength, which gives them the potential as a reinforcing material. The whiskers are very small (length 50–70 μm, diameter 1–3 μm). It is therefore not possible to measure their mechanical properties directly. Tashiro calculated the Young's modulus of the fully extended PHB chain in a polymer single crystal to 157 GPa.[8] The whiskers have a low density (1.5 g cm^{-3}) and a high thermal stability with a decomposition temperature of about 500°C.

Commercial polyamides are often reinforced with short fibers. Disadvantages in using commercial glass fibers are the enhancement of the viscosity of the material by the addition of the fibers. Its content has to be more than 30% to reach an acceptable reinforcing effect. This leads to difficulties during processing of the composites.[10] It is therefore of interest to find alternatives for the conventional short fibers, which can be PHB whiskers. In this article, two polyamides, polyamide-6 and polyamide-11, were used as the matrix polymers for PHB whisker/polyamide composites. The reinforcement efficiency of the whiskers was investigated with respect to the whisker content, the aspect ratio of the whiskers,

* To whom correspondence should be addressed.

Journal of Applied Polymer Science, Vol. 61, 783–792 (1996)
 CCC 0021-8995/96/050783-10

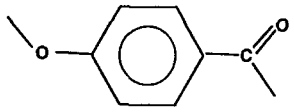

Figure 1 Structural formula of poly(4-hydroxybenzoate).

and the properties of the polyamide matrices via tensile testing and scanning electron microscopy.

EXPERIMENTAL

PHB whiskers with an average aspect ratio, l/d, of 50 and PHB slablike crystals, also called "PHB slabs," with an l/d of 1, were kindly supplied by Kricheldorf and co-workers (see Ref. 6). To remove solvent residues, the whiskers and slabs were extracted with acetone for 2 days in a Soxhlet extractor and dried in a vacuum for 4 h at 100°C.

Polyamide-6 (PA-6) (Ultramid S3) was provided by the Bayer Chemical Co. Polyamide-11 (PA-11) was purchased from Polyscience Ltd. Both polymers were dried at 77°C in a vacuum for 6 h before use.

The composites were prepared by mixing the whiskers into the melt of the matrix polymer. The mixing procedure was carried out with a spatula on a heated plate. For preparation of the PA-6 composites, a temperature of 270°C was chosen. The temperature for the preparation of the PA-11 was 240°C. The whisker volume fraction, V_f, in the PA-6 composites varied as 2, 5, 10, and 20 vol %, and in the PA-11 composites, as 2, 5, 15, 30, and 50 vol %.

The composite materials were consolidated in a heated press above the melting temperature of the polyamides (240°C for PA-6, 200°C for PA-11) to films of a thickness of 0.1–0.5 mm, followed by rapid quenching between two metal plates, down to −20°C in the case of the polyamide-6 composites and to +20°C in the case of the PA-11 composites. In the case of the PA-6 composites, one set of films was annealed after quenching to 160°C for 2 h. From the films, dog bone-shaped tensile test specimens with a gauge length of 20 mm and a width of 4 mm were cut.

Tensile tests were carried out in a Zwick 1445 at a crosshead speed of 1 mm/min. Scanning electron microscopy (SEM) was performed with a Leitz 1600T. The samples for SEM investigation were sputtered with a 20 nm layer of gold. The density, ρ, of the materials was determined by weight measurements of the specimens in air and in petrol ether 40/60 with a pygnometer.

RESULTS AND DISCUSSION

Tensile Properties of the Composites

The reinforcement efficiency of the PHB whiskers in the polyamide matrix was investigated by tensile testing. This gives information about the enhancement of the elastic modulus, the yield stress, and the fracture stress of the respective matrices with respect to their whisker content. The chemical and the mechanical properties of the polyamide matrix was varied in order to investigate the influence of the different properties on the reinforcement efficiency of the PHB whiskers.

In the PA-6 composites, the ductility was varied by different heat treatments of the samples, as already described above. The PA-6 in the quenched samples has a relatively low crystallinity, leading to a low elastic modulus (E_m = 500 MPa) and a high fracture strain (ε_r = 470%), the so-called "ductile PA-6 composites." The PA-6 in the annealed samples instead has a higher crystallinity, leading to a higher stiffness (E_m = 1000 MPa) and a lower fracture strain (ε_r = 46%), called the "stiff PA-6 composites."

The chemical properties of the matrices were varied by choosing two different frequencies of the amide groups in the polymer chain, which means that a second polyamide, PA-11, was chosen. It is expected that the amide groups are able to form hydrogen bonds to the carbonyl groups of the whiskers and therefore strongly influence the whisker/matrix adhesion, as illustrated in Figure 3.

The whiskers were statistically oriented in the samples. In the PA-6 composite, agglomerates of whiskers, due to an incomplete mixing of the components during the preparation, can be observed

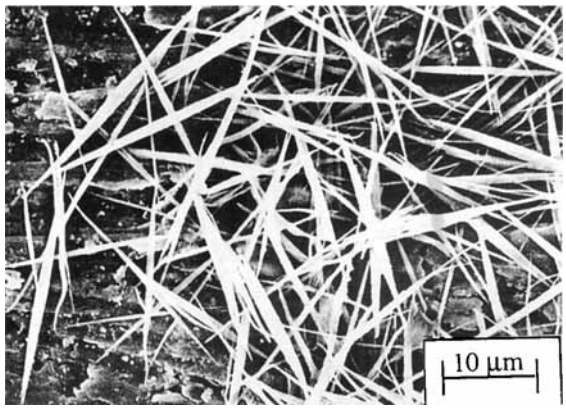

Figure 2 Scanning electron micrograph of PHB whiskers.

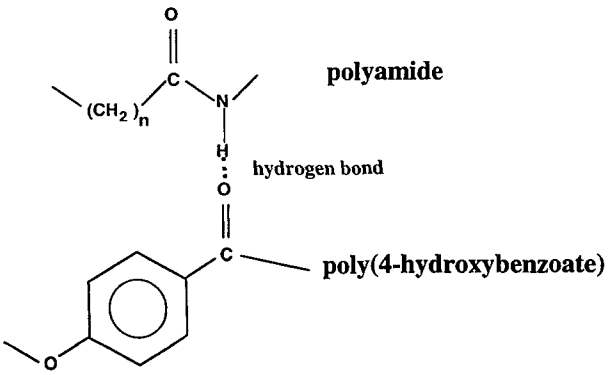

Figure 3 Hydrogen bond between polyamide and PHB (schematically).

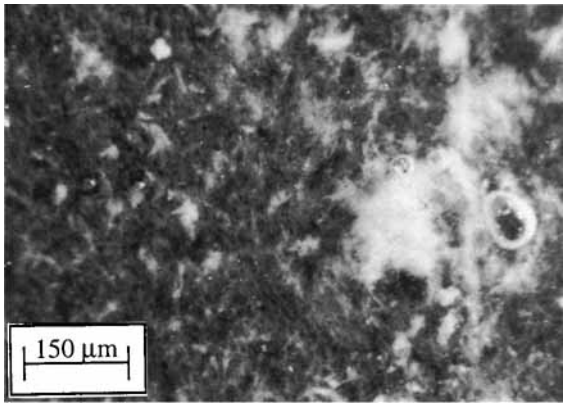

Figure 4 Micrograph of PHB whisker/PA-6 composites.

(Compare Fig. 4). In the PA-11 composite, the distribution of the whiskers is much more homogeneous (see Fig. 5), because of the much easier mixing of the matrix material with the whiskers.

In Table I are summarized the elastic modulus, the yield stress, the fracture stress, and the fracture strain of each composite. Figure 6(a)–(d) shows the relative tensile properties of the composites compared to the respective pure matrix, i.e., E/E_m, σ_f/σ_{fm}, σ_r/σ_{rm}, and $\varepsilon_r/\varepsilon_{rm}$ with respect to their whisker volume fraction V_f.

To compare the reinforcement efficiency of the PHB whiskers in the different composites, i.e., the relative change of the tensile modulus E and the yield stress σ_f with increasing whisker volume fraction, V_f, several theoretical approaches could be used.[11] We chose the Halpin–Tsai equation, modified by Nielson, which is common practice for short-fiber composites [eq. (1)]. It relates the elastic modulus of a composite E to the modulus of the matrix E_m, the elastic modulus of the reinforcement E_f, and its aspect ratio l/d. If two different matrices with equal elastic moduli are reinforced with the same fibers, the results should be equal, according to the Halpin–Tsai-equation. The differences, measured in reality, can be valued as different reinforcing efficiencies of the fibers in the composites, which are compared. Therefore, the reinforcing efficiencies of fibers in different composites, in which the elastic moduli of the matrices are equal, can be directly compared by plotting the elastic modulus vs. the fiber volume fraction for each composite system.

In the composites, used in this study, the elastic moduli of the matrices (ductile and stiff PA-6, PA-11) are not equal. But the differences between the values for the elastic moduli of different matrices, as an example, [E_m(ductile PA-6) − E_m(PA-11)], do not influence significantly the expected reinforcement effects caused by the whiskers. As an example, the relative enhancement of the elastic modulus of the ductile PA-6 by the addition of 2% PHB whiskers is E/E_m = 1.62, according to the Halpin–Tsai equation. The elastic modulus of the pure PA-6 is 500 MPa. The same whisker content in PA-11, which has an elastic modulus of 580 MPa, should lead to a reinforcement effect (E/E_m) of 1.59, according to the Halpin–Tsai equation. The difference between 1.62 and 1.59 is in the range of the standard deviation of the measured values for E/E_m. Therefore, the reinforcement efficiency of the whiskers in the different composites, concerning the enhancement of the elastic modulus of the respective matrix, can be directly compared by plotting the relative elastic modulus E/E_m vs. the whisker volume fraction V_f for each composite. For the yield stress σ_f of a short-fiber composite, an equation, analogous to the Halpin/Tsai/Nielson equation, was formulated.[12] Therefore, the same arguments are valid for the yield stresses of the composites.

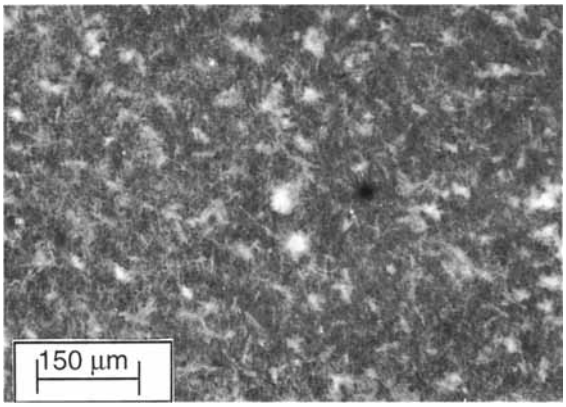

Figure 5 Micrograph of PHB whisker/PA-11 composites.

Table I Tensile Properties PHB Whisker/Polyamide Composites

PA (V_f [%])	E [MPa]	σ_f [MPa]	σ_r [MPa]	ϵ_r [%]
Ductile PA-6				
[0]	500 ± 70	6.0 ± 1.0	56 ± 10	470 ± 100
[2]	1100 ± 80	11.8 ± 0.2	32 ± 5	10 ± 3
[5]	1080 ± 100	12.3 ± 0.1	35 ± 9	15 ± 3
[10]	1150 ± 60	12.0 ± 0.5	36 ± 3	10 ± 3
[20]	980 ± 50	9.8 ± 0.6	18 ± 3	2.3 ± 0.5
Stiff PA-6				
[0]	1000 ± 80	16.9 ± 2.8	41 ± 4	46 ± 2
[2]	1480 ± 110	22.0 ± 2.7	39 ± 7	7 ± 5
[5]	1200 ± 100	23.0 ± 2	37 ± 7	8 ± 3
[10]	1370 ± 70	14.3 ± 0.6	33 ± 6	7 ± 2
[20]	1400 ± 120	13 ± 1	26 ± 5	5.0 ± 0.9
PA-11				
[0]	580 ± 20	8 ± 3	42 ± 10	300 ± 80
[2]	810 ± 70	12.2 ± 0.5	34 ± 7	90 ± 40
[5]	780 ± 40	10.2 ± 0.5	26 ± 8	140 ± 30
[15]	1270 ± 40	12.3 ± 0.6	25 ± 6	8 ± 3
[30]	1280 ± 50	17.4 ± 0.8	29 ± 4	5 ± 1
[50]	1580 ± 50	13 ± 1	16 ± 3	3.5 ± 1

In Figure 6(a), the relative elastic modulus E/E_m of the PA-6 and the PA-11-composites is plotted vs. the whisker volume fraction V_f. The ductile PA-6 composites show a sharp increase in E/E_m with increasing V_f at low whisker contents. A similar behavior is observed in the case of the relative yield stress σ_f/σ_{fm} of the ductile PA-6-composites [Fig. 6(b)]. The behavior of the stiff PA-6 composites is similar to the behavior of the ductile PA-6 composites, but the increase in E/E_m and σ_f/σ_{fm} is not as pronounced as in the ductile PA-6 composites. In the case of the PA-11 composites, the increase in E/E_m and σ_f/σ_{fm} is much lower than in the ductile PA-6 composites and also lower than in the stiff PA-6 composites [see also Fig. 6(a,b)] when the whisker volume fraction is lower than 10%.

The different behaviors of the PA-6 composites and the PA-11 composites at low whisker contents can be explained by the different chemical structures of PA-6 and PA-11, i.e., their different amide group frequency. In PA-6, there are more amide groups per matrix volume, which are able to form hydrogen bonds to the carbonyl or other functional groups on the whisker surface. Therefore, the whisker–matrix adhesion is expected to be essentially better in the PA-6 composites than in the PA-11 composites, leading to a better stress transfer from the matrix into the whiskers and, further, to better tensile properties.

At higher whisker volume fractions (above 10%), the increase in E/E_m and σ_f/σ_{fm} in the PA-6 composites decreases, and there is even a decrease of σ_f/σ_{fm} in the case of the stiff PA-6 composites. In contrast, the PA-11 composites show a steady increase of E/E_m and σ_f/σ_{fm} even at whisker volume fractions above 30%. These different behaviors compared to the PA-6 composites can be explained by different failure mechanisms in the respective composites. In the PA-6 composites, there are agglomerates of whiskers, which are mechanical weak points due to whisker–whisker attachments and because the wetting of the whiskers with the matrix in between the agglomerates is worse than in the case of a homogeneous distribution of the whiskers. This leads to an early failure of the material, because in the agglomerates, an early crack growth is initialized due to stress concentrations. In the PA-11 composites, the distribution of the whiskers is more homogeneous and therefore also the stress distribution within the material is more homogeneous.

Therefore, the fracture strain ϵ_r/ϵ_{rm} sharply decreases in the PA-6 composites even at low whisker volume fractions [Fig. 6(d)]. This is less pronounced in the PA-11 composites with a smoother decrease of ϵ_r/ϵ_{rm}. This indicates that the strain of the PA-11 matrix is less influenced by the whisker content and that high stress concentrations, which would lead to an early failure of the material, are not generated.

In Figure 6(c), the relative fracture stresses σ_r/σ_{rm} of the different composites are plotted vs. the whisker volume fraction. The decrease of σ_r/σ_{rm} can

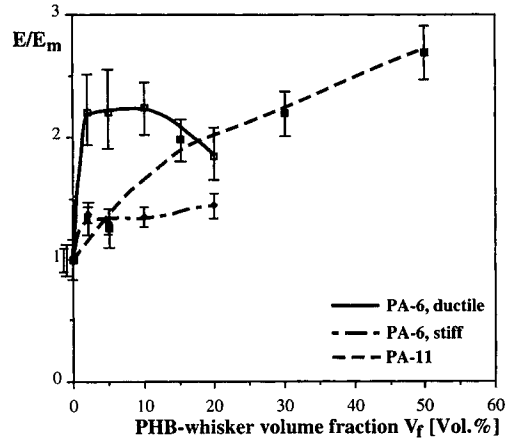

Fig. 6a

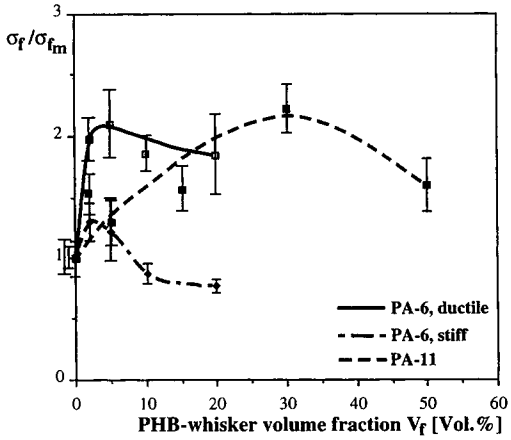

Fig. 6b

Figure 6 (a–d) Relative elastic modulus E/E_m, yield stress σ_f/σ_{fm}, fracture stress σ_r/σ_{rm}, and fracture strain $\varepsilon_r/\varepsilon_{rm}$ of the PHB whisker/polyamide composites as a function of the PHB whisker volume fraction V_f.

also be explained by the different failure mechanisms, mentioned above, and by the fact that the high elongation of the matrix leads to a preferred orientation, causing a higher strength than in the nonoriented matrix. Therefore, the composites with low fracture strains also possess small fracture stresses compared to the respective elongated pure matrix.

Morphology of the Fracture Surface

After tensile testing, the fracture surfaces were examined by scanning electron microscopy (SEM). Figure 7 shows a fracture surface of a ductile PA-6 composite with a whisker volume fraction of 5%: Whiskers are pulled out of the matrix. At the bottom, the whiskers are covered by a conus of matrix material (indicated by arrows in Fig. 7). This can be explained by the model, schematically shown in Figure 8: A crack, propagating through the composite, touches and circumferizes the whisker. Then, the whisker is pulled out of the matrix. During the pull-out process, two coni are formed on the corresponding fracture surfaces, where the crack has circumferized the whisker. This can be explained by the fact that the matrix, which is attached to the whisker, is deformed into the pulling direction due to the whisker–matrix adhesion. These morphological effects are consistent with the mechanical behavior of the ductile PA-6-composites, which indicates relatively good adhesion properties.

In the stiff PA-6 composites, another failure mechanism is observed: The samples are more brittle at the interspherulitic boundaries (see SEM micrograph, Fig. 9). The ductility of the matrix is not high enough to form a conus at the bottom of the whisker during the pullout process.

In the PA-11 composites, the matrix shows a strong plastic deformation even at higher whisker volume fractions, which can be seen in the SEM micrograph (Fig. 10), where the plastically deformed areas of the matrix are indicated by arrows. This is in agreement with the fact that the fracture strain

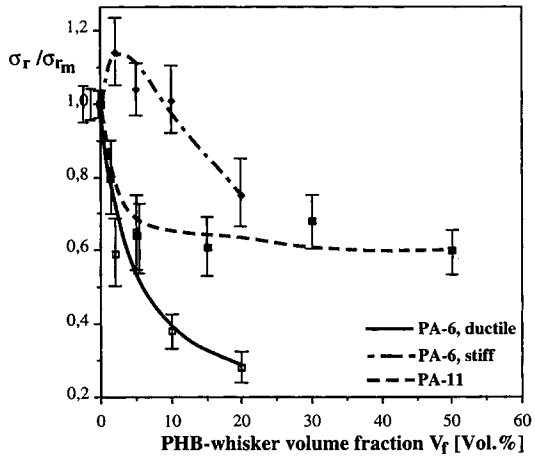

Fig. 6c

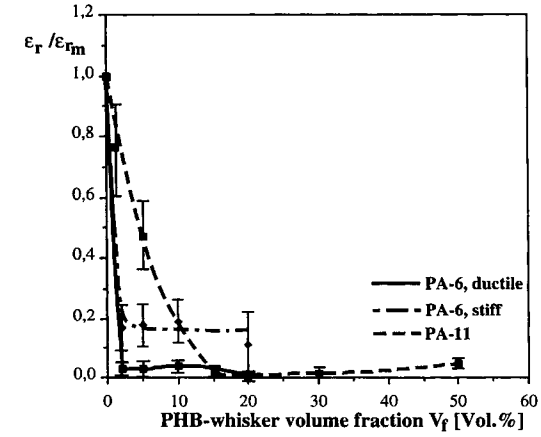

Fig. 6d

Figure 6 (*Continued*)

$$\frac{E_L}{E_1} = \frac{1 + 2(l/d)B_L V_f}{1 - B_L V_f}; \quad B_L = \frac{E_2/E_1 - 1}{E_2/E_1 + 2(l/d)}$$

$$\frac{E_T}{E_1} = \frac{1 + 2B_T V_f}{1 - B_T V_f}; \quad B_T = \frac{E_2/E_1 - 1}{E_2/E_1 + 2}$$

$$\boxed{\frac{E_R}{E_1} = \tfrac{3}{8}E_L + \tfrac{5}{8}E_T}$$

E_2 Modulus of the reinforcing fibers
E_1 Modulus of the matrix
V_f Volume fraction of the reinforcing fibers
l/d Aspect ratio of the reinforcing fibers
E_L Modulus of the composite in fiber direction
E_T Modulus of the composite perpendicular to the fiber direction
E_R Modulus of the composite with a statistical dispersion of the fibers

Equation (1) Nielson/Halpin–Tsai equation.

is relatively high even at higher whisker volume fractions. The whiskers are also pulled out of the matrix, but the formation of a conus as in the ductile PA-6 composites cannot be observed. This also is an indication of a much weaker adhesion than in the PA-6 composites. It is also consistent with the lower increase in E/E_m and σ_f/σ_{fm} with increasing whisker volume fraction, when compared to the PA-6 composites.

Density Measurements

To check the influence of the PHB whiskers on the crystallization of the matrices, the densities of the materials were measured. From the measured densities of the composites, the densities of the matrix

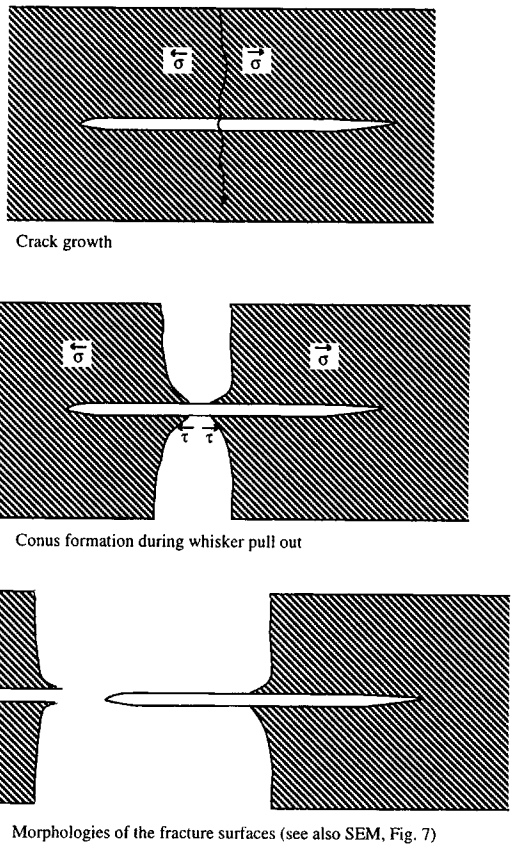

Figure 8 Model for the formation of the fracture surface in PHB whisker/ductile PA-6 composites (schematically).

can be calculated, using eq. (2). The density of the matrices is linearly correlated with the crystallinity.

In Figure 11, the densities of the matrices are plotted vs. the respective whisker volume fractions, V_f. If the whiskers would act as a nucleating agent for the crystallization of the matrix, an increase in crystallinity can be expected and, therefore, also the

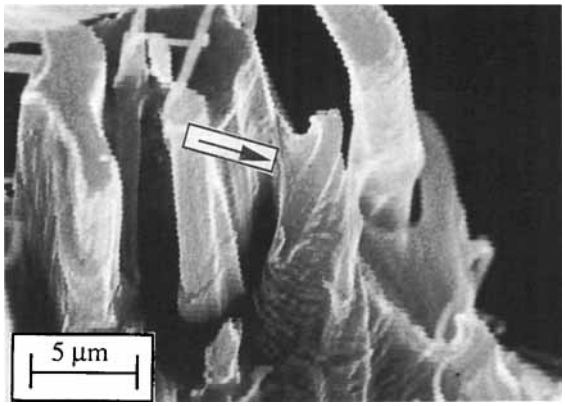

Figure 7 Scanning electron micrograph of the fracture surface of PHB whisker/ductile PA-6 composites.

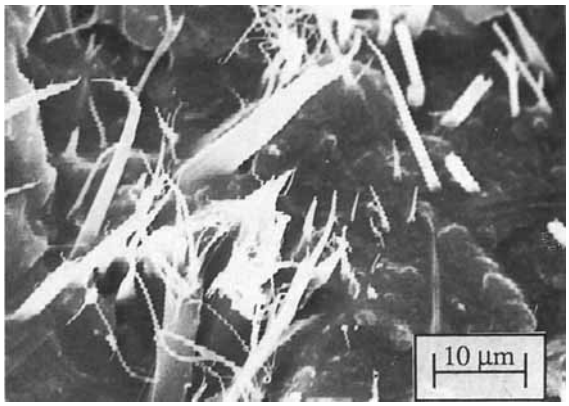

Figure 9 Scanning electron micrograph of the fracture surface of PHB whisker/stiff PA-6 composites.

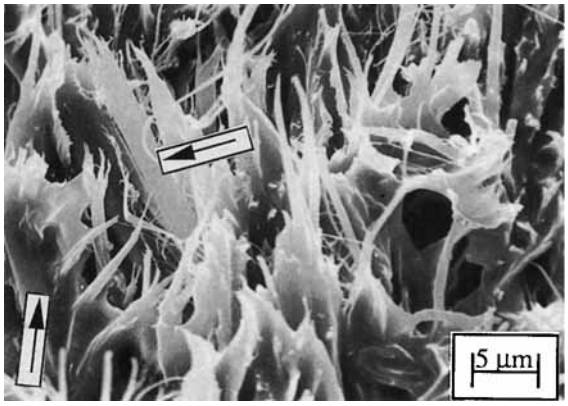

Figure 10 Scanning electron micrograph of the fracture surface of PHB whisker/PA-11 composites.

density of the matrix would increase with increasing whisker volume fraction. However, a decrease of the densities of the respective matrices with increasing whisker volume fraction was determined. This could be due to the inclusion of air, but they are not visible in the light microscope; consequently, a decrease of the crystallinity has to be assumed.

The reinforcement effects, measured in the systems investigated, can therefore solely be reduced to the influence of the whiskers in the composites. An enhancement of the crystallinity by the addition of the whiskers, which alone would lead to an increase in the elastic modulus and yield stress without a reinforcement effect caused by the whiskers, is not observed.

Influence of the Aspect Ratio of the PHB

Another subject of investigation was the influence of the aspect ratio l/d of the PHB single crystals on the reinforcement efficiency. Therefore, PHB slablike crystals, shown in Figure 12, were additionally used for the preparation of PHB slablike crystal/ductile PA-6- and PA-11 composites. In the

$$\rho_{PA}^{X_{PA}} = \rho_{PHB} - \frac{\rho_{PHB} - \rho_{Exp.}}{X_{PA}}$$

$\rho_{Exp.}$ Measured density of the composite
ρ_{PHB} Density of the poly(4-hydroxybenzoate) whiskers
X_{PA} Weight fraction of the polyamide matrix
$\rho_{PA}^{X_{PA}}$ Density of the polyamide in the composite

Equation (2) Relationship between the density of a composite and the density of the respective matrix content.

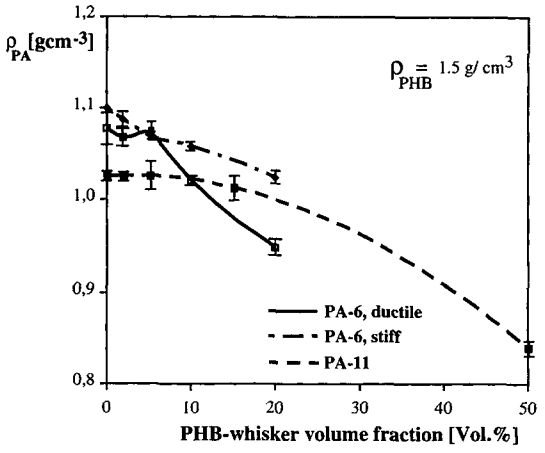

Equation 2

$$\rho_{PA}^{X_{PA}} = \rho_{PHB} - \frac{\rho_{PHB} - \rho_{Ges}}{X_{PA}}$$

Figure 11 Density ρ_{PA} of the polyamides in the PHB whisker/polyamide composites as a function of the whisker volume fraction V_f.

PHB slablike crystals, the chain direction is perpendicular to the top surfaces of the slabs. PHB slabs, 2 and 5 vol %, were added to PA-6 in order to compare these composites with the respective PHB whisker/ductile PA-6 composites. The PHB slablike crystal volume fractions V_{sl}, chosen for the PA-11 composites, were 15 and 30 vol %. The tensile properties of the PHB slablike crystal composites are summarized in Table II. In Figure 13(a–d), their relative tensile properties, i.e., E/E_m, σ_f/σ_{fm}, σ_r/σ_{rm}, and $\varepsilon_r/\varepsilon_{rm}$, are plotted vs. the PHB slablike crystal volume fraction V_{sl}.

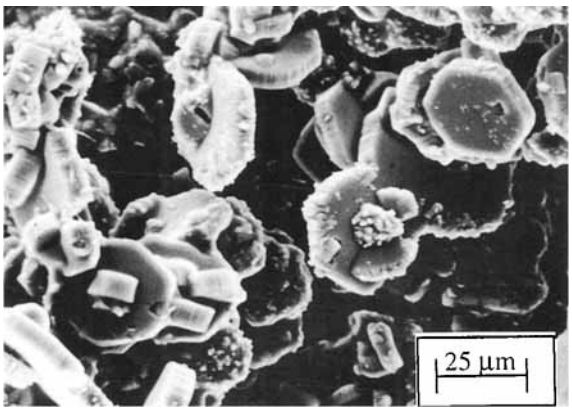

Figure 12 Scanning electron micrograph of PHB slablike crystals.

Table II Tensile Properties PHB Slablike Crystal/Polyamide Composites

PA (V_s [%])	E [MPa]	σ_f [MPa]	σ_r [MPa]	ϵ_r [%]
Ductile PA-6				
[0]	500 ± 70	6.0 ± 1.0	56 ± 10	470 ± 100
[2]	608 ± 70	9.3 ± 1.2	36 ± 6	200 ± 110
[5]	620 ± 50	9.6 ± 4.0	30 ± 3	190 ± 65
[20]	870 ± 170	12 ± 2.0	31 ± 5	21 ± 5
PA-11				
[0]	580 ± 20	8 ± 3	42 ± 10	300 ± 80
[15]	754 ± 60	14.0 ± 1.5	29 ± 3	12 ± 3
[30]	986 ± 150	14.4 ± 1.5	31 ± 7	10 ± 1

In the PHB slablike crystal/ductile PA-6 composites [black line in Fig. 13(a–d)], the enhancement of the relative tensile modulus E/E_m and the relative yield stress σ_f/σ_{fm} at low PHB content is less pronounced than in the respective PHB whisker composites. At higher PHB slab volume fractions, the increase in E/E_m and σ_f/σ_{fm} levels off, but there is no decrease as in the respective PHB whisker composites [compare Fig. 6(a,b) and Fig. 13(a,b)]. This is due to the much more homogeneous distribution of the PHB slabs in the matrix in contrast to the respective whisker composites, as to be seen in the photographs (Figs. 14 and 15). Consistent with these observations are the curvatures of the relative fracture stresses σ_r/σ_{rm} and the relative

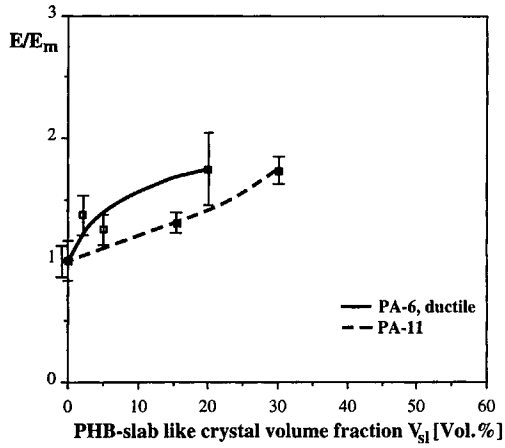

Fig. 13a

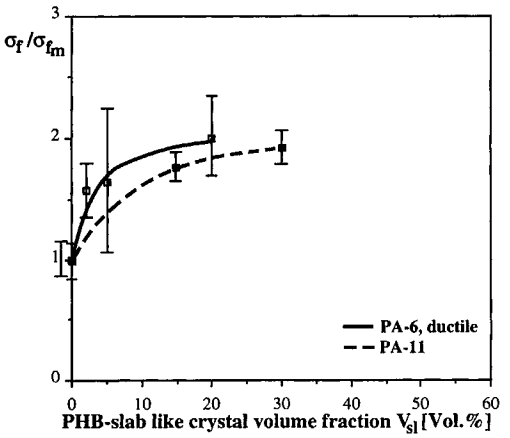

Fig. 13b

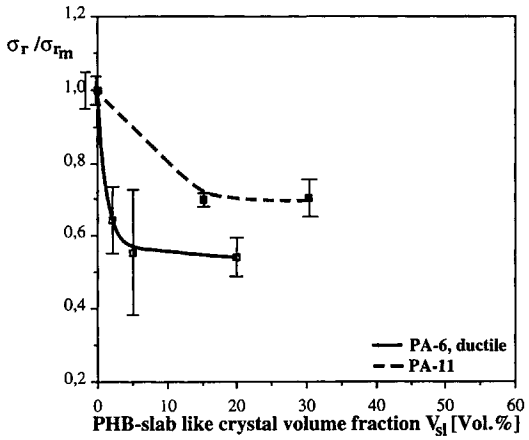

Fig. 13c

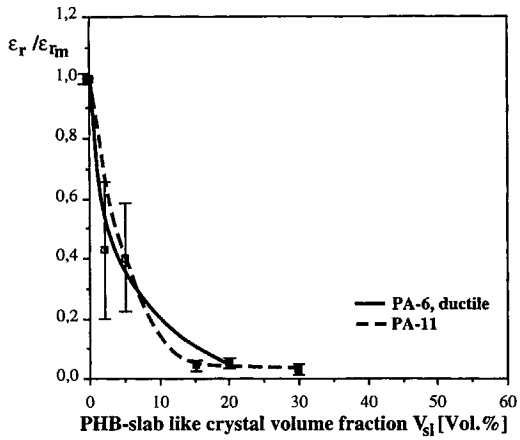

Fig. 13d

Figure 13 (a–d) Relative elastic modulus E/E_m, yield stress σ_f/σ_{fm}, fracture stress σ_r/σ_{rm}, and fracture strain ϵ_r/ϵ_{rm} of the PHB slablike crystal/polyamide composites as a function of the PHB slablike crystal volume fraction V_{sl}.

Figure 13 (*Continued*)

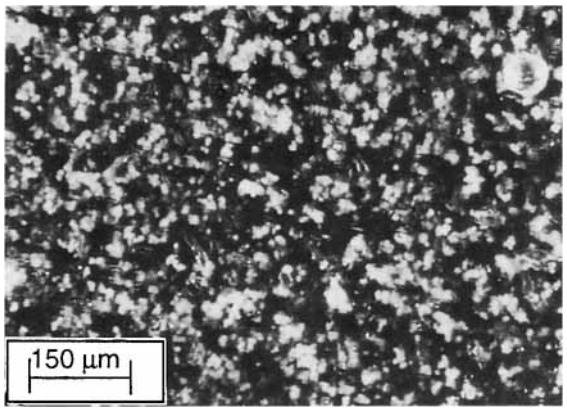

Figure 14 Micrograph of PHB slablike crystal/PA-6 composites.

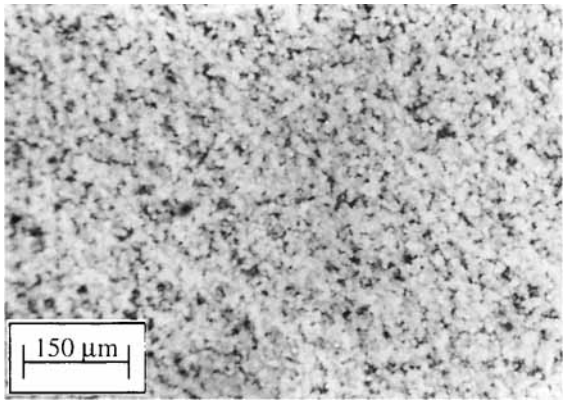

Figure 15 Micrograph of PHB slablike crystal/PA-11 composites.

fracture strains $\varepsilon_r/\varepsilon_{rm}$ with increasing PHB slab volume fraction: The decrease in σ_r/σ_{rm} and $\varepsilon_r/\varepsilon_{rm}$ with increasing PHB content is lower than in the respective whisker composites, because there are no mechanical weak points in the PHB slab composites like in the PHB whisker/PA-6 composites.

In the PHB slablike crystal/PA-11 composites (red line in Fig. 13(a–d)], the increase in E/E_m and σ_f/σ_{fm} is lower than in the PHB slablike crystals/PA-6 composites, which could have been expected, because the adhesion between PHB and PA-11 is weaker. Compared to the PHB whisker/PA-11 composites, the increase of E/E_m is lower in the slablike crystal/PA-11 composites, but the increase in σ_f/σ_{fm} is nearly equal in both composites. An explanation cannot be given. σ_r/σ_{rm} and $\varepsilon_r/\varepsilon_{rm}$ behave in a similar way, as in the respective whisker composites, indicating that in the PA-11 composites the PHB whiskers and the PHB slabs are more homogeneously distributed than in the PA-6 composites.

An SEM micrograph of the fracture surfaces of the PHB slablike crystal/ductile PA-6 composites is shown in Figure 16. On the top surfaces of the slabs, microfibrils are visible. It is not detectable whether the fibrils are generated from matrix material or from the PHB slabs. Slabs, which are oriented with their top surface perpendicular to the tensile direction, seem to be broken perpendicularly to the chain direction. This could explain the fibrillation on these surfaces: The attractive interactions between the chains in the lamellae are weak compared to the chemical bonds parallel to the chain direction. In consequence, the lamellae can easily be broken by tensile stresses perpendicular to the chain direction. Mechanistically, bundles of chains are pulled out of the lamellae, so that microfibrils are formed.

The fracture surfaces of the PHB slablike crystal/PA-11 composites show similar phenomena (Fig. 17). Fibrillations are visible as well, but they seem mostly to be generated from the matrix, which covers the PHB slabs. Slabs are partially visible on the fracture surface. They seem to be unaffected by the tensile stresses, except some fibrillations, which are originating from the slabs, as there are kink bands visible (arrows in Fig. 17). These facts are consistent with the assumption that the adhesion between PHB and PA-11 is much weaker than is the adhesion between PHB and PA-6.

In future investigations, we will try to modify the surface properties of the PHB whiskers, in order to enhance the adhesion properties to polyamide and other thermoplastic matrices, which could lead to whisker breakage during tensile testing, in contrast to the pullout mechanisms, observed in the here-investigated composites. In that case, the whole strength of the PHB whiskers could be used for the

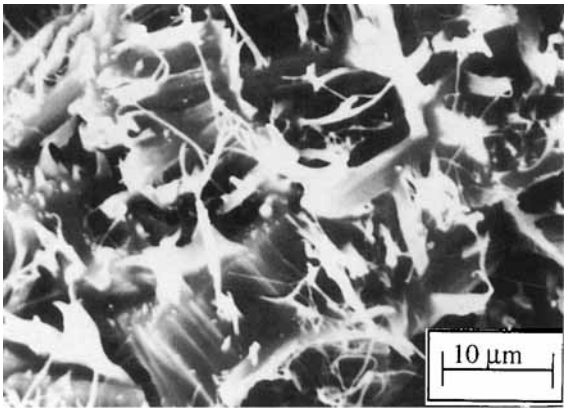

Figure 16 Scanning electron micrograph of the fracture surface of PHB slablike crystal/ductile PA-6 composites.

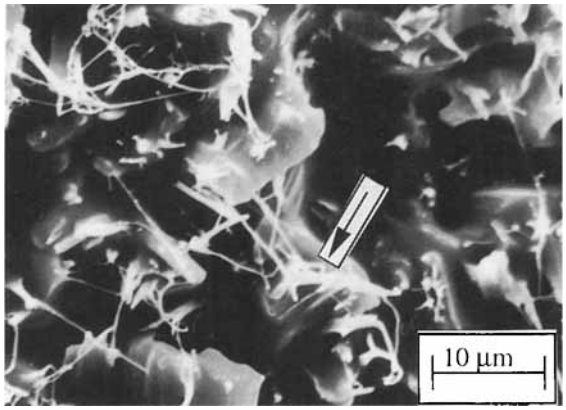

Figure 17 Scanning electron micrograph of the fracture surface of PHB slablike crystal/PA-11 composites.

reinforcement of the matrix material. A further enhancement of the aspect ratio of the whiskers could improve the reinforcement efficiency, too, if the critical fiber length can be reached in some matrices.

Financial support was kindly given by the DFG in the Project A3 of the SFB 371.

REFERENCES

1. J. Economy, S. G. Nowak, and S. G. Cottis, *SAMPE J.*, **6**, 6 (1970).
2. G. Lieser, *J. Polym. Sci. Polym. Phys. Ed.*, **21**, 1614 (1983).
3. H. R. Kricheldorf and G. Schwarz, *Polymer*, **25**, 520 (1984).
4. Y. Yamashita, *Makromol. Chem. Rapid Commun.*, **9**, 687 (1988).
5. H. R. Kricheldorf and G. Schwarz, *Polymer*, **31**, 481 (1990).
6. H. R. Kricheldorf, F. Ruhser, G. Schwarz, and T. Adebahr, *Makromol. Chem.*, **192**, 2371 (1991).
7. C. Taesler, J. Petermann, H. R. Kricheldorf, and G. Schwarz, *Makromol. Chem.*, **192**, 2255 (1991).
8. K. Tashiro, *Polymer*, **32**(3), 454 (1991).
9. H. R. Kricheldorf, F. Ruhser, and G. Schwarz, *Macromolecules*, **24**, 4990 (1991).
10. J. Karger-Kocsis and K. Friedrich, in *Advancing with Composites Conference*, Milan, May 1988, I. Crivelli Visconti, Ed., CUEN, Milan, 1988, p. 639.
11. L. E. Nielson, *J. Appl. Phys.*, **41**, 4626 (1970).
12. L. E. Nielson, *Mechanical Properties of Polymers and Composites*, Vol. 2, Marcel Dekker, New York, 1974.

Received November 27, 1995
Accepted January 31, 1996